International Journal of Basic and Applied Sciences, 14 (1) (2025) 445-452

International Journal of Basic and Applied Sciences

Website: www.sciencepubco.com/index.php/IJBAS
https://doi.org/10.14419/fwg9s764
Research paper

Antioxidant efficacy of synthesized composite copper lutein nano nutraceuticals from brassica oleracea var italica

Saif Saadee Nawaf [1] *, Sudhakar Malla [2], Manjula Ishwara Kalyani [3]

[1] *Department of Biotechnology, Mangalore University, Mangalagangothri, Mangalore*
[2] *Department of Microbiology, Mangalore University, Jnana Kaveri, Chikka Aluvara, Kodagu*
[3] *Insearch Biotech laboratory, Bangalore*
**Corresponding author E-mail: s88aif@gmail.com*

Received: April 15, 2025, Accepted: May 21, 2025, Published: May 2 7, 2025

Abstract

Aim: Due to its antioxidant properties, lutein scavenges reactive oxygen species, including lipid peroxy radicals and singlet oxygen. Despite the therapeutic promise derived from its various physiological functions, lutein's absorption and stability issues make efficient distribution challenging. Nanotechnology applications in pharmaceuticals have been the subject in recent decades. Similar to nanopharmaceuticals, a new class of nanomaterials known as nanonutraceuticals has evolved due to the application of nanotechnology for improved nutraceutical delivery.
Methods: For green synthesis, B. oleracea stalks and florets were utilized individually in a copper sulphate solution. The synthesized Copper nanoparticles were characterized and screened for their antibacterial and anti-biofilm activities.
Results: At 400µg/ml concentrations, FLNP and FNP demonstrated 92 and 88% DPPH free radical scavenging, respectively. Comparing the different NPs to the positive control, FLNP demonstrated the highest H2O2 scavenging activity (IC50 72.55µg/ml), followed by FNP. When compared to the positive control, FLNP, FNP, and Lutein demonstrated antioxidant capacities of 94, 91, and 87% at 400µg/ml using the reducing power method. According to our ferrozine assay results, FLNP demonstrated an efficient ability to bind iron, suggesting that this property may be linked to its antioxidant properties. According to their different antioxidant capacities, FLNP and FNP demonstrated 92 and 88% FZ reduction ability.
Conclusion: The present study was successful in synthesizing composite lutein-based copper nanoparticles and also confirmed of the potential antioxidant activity exhibited by the composite particles. The composite particles did exhibit enhanced antioxidant activity when compared to other controls.

Keywords: *Copper Nanoparticles; Broccoli; FTIR; Antioxiants; Lutein; DPPH; Ferrozine Assay; RP Method.*

1. Introduction

Malnutrition is a serious health concern in developing nations and is a poor prognostic indicator for several diseases. Numerous critical physiological processes, such as gene transcription, signalling transduction, and immunological response, are influenced by reactive oxygen species (ROS). Superoxide ($O_2^{\bullet-}$), hydrogen peroxide (H_2O_2), and hydroxyl radicals (•OH) are examples of common ROS (Rogers et al., 2014). Oxidative damage to biomolecules, including lipids, proteins, and DNA, can be caused by an excess of ROS and has been linked to aging as well as several illnesses, including cancer, cardiovascular and and digestive disorders (Zuo et al., 2015). Excess ROS shows harmful consequences that sometimes lead to mortality (Muller and Krawinkel, 2005).
According to Harman's 1956 free radical hypothesis, aging is a process associated with a cumulative and irreversible build-up of oxidative damage (Mariani et al., 2005).
As cells age, the GSH/GSSG ratio decreases, due to a change in redox balance. The cellular capacity to buffer ROS generated both naturally and in response to external stress may be compromised by this change in the redox profile. Overproduction of ROS can directly harm lipids, proteins, and DNA, disrupting regular physiological processes (Zuo et al., 2015).
Particularly vulnerable to OS is mitochondrial DNA (mtDNA), and aging has been intimately associated with mtDNA mutation (Trifunovic et al., 2004). According to one study, mice with somatic mtDNA mutations lived shorter and showed early symptoms of osteoporosis and hair loss. According to Kregel and Zhang (2007), exposure to elevated ROS levels can also hasten telomere shortening, which eventually leads to cellular senescence. Fibroblast cells cultivated under high OS, for instance, had a shorter lifespan and a higher rate of telomere shortening. Furthermore, via activating NF-κB, aging-associated OS may be the cause of the persistent, systemic inflammation frequently observed in the elderly. According to Chung et al. (2009), NF-κB is a crucial regulator of cytokines like interleukin (IL)-1β, IL-6, and tumor necrosis factor-alpha (TNF-α). Unlike chronic activation during aging, OS-induced NF-κB signaling is transient under normal

Copyright © Saif Saadee Nawaf et al. This is an open access article distributed under the Creative Commons Attribution License, which permits unrestricted use, distribution, and reproduction in any medium, provided the original work is properly cited.

circumstances (Chung et al., 2009). Age-related illnesses like dementia, cancer, and atherosclerosis may arise as a result of the ongoing low-level inflammation.

Due to a general deterioration in bodily functions, such as a lower metabolic rate, digestive capacity, and absorption capacity, older populations are more susceptible to malnutrition (Brownie, 2006). As a result, diseases linked to inadequate nutrition are more likely to strike the elderly. Since the food is a vital source of exogenously derived antioxidants, attention has been focused more on it in recent years. By inhibiting the production of free radicals, dietary antioxidants seem to have anti-aging properties (Kandola et al., 2015). One of the main health issues facing the aging population is cognitive decline.

In a seminal study, Kang et al. (2005) tracked 10,000 women between 1984 and 2003 to examine the connection between their food habits and cognitive abilities. According to research, women who ate more cruciferous or green leafy vegetables showed the least amount of cognitive deterioration, whereas fruit consumption did not affect their cognitive abilities (Kang et al., 2005). It's interesting to note that, after controlling for age, BMI, smoking status, and sun exposure, Japanese women who consumed more green and yellow vegetables also had slower skin aging rates (Nagata et al., 2010).

The accumulation of several events in a single cell is what defines the genesis of cancer. Three stages—initiation, promotion, and progression—can be used to characterize it. ROS is a part of all these phases. The kind and reactivity of the radicals involved directly correlate with the impact of oxidative stress at a particular stage of carcinogenesis. An initiated cell is produced when a normal cell sustains a DNA mutation that, when followed by a round of DNA synthesis, fixes the mutation (Trachootham D, 2008). The presence of oxidative DNA alterations in cancer tissues supports the idea that ROS might cause cancer. Clonal growth of started cells, induction of cell proliferation, and/or prevention of apoptosis are characteristics of the promotion stage. At this point, oxidative stress plays a significant role. By momentarily altering the genes linked to cell death or proliferation, ROS can promote the growth of mutant cell clones (Valko M, 2006).

Lutein is a yellow-orange pigment that is commonly found in plants and is a member of the xanthophyll family of carotenoids. Dietary sources of lutein include dark leafy greens like spinach and kale, as well as yellow-colored foods like corn and egg yolks (Ahn, Y.J., 2021). Lutein is thought to have anti-inflammatory, antioxidant, and anti-proliferative properties (Eliassen, A.H., 2012). ROS activates inflammatory signaling, which leads to the development of metabolic and inflammatory diseases. Lutein maintains endogenous antioxidant glutathione and promotes expression of antioxidant enzymes like catalase, superoxide dismutase, and glutathione peroxidase. to reduce ROS levels (Eliassen, A.H, 2015).

Accordingly, lutein also helps prevent oxidative stress-related diabetic retinopathy, cardiovascular diseases, and neurodegenerative disorders (Kim, J.H., 2018). Epidemiological studies show that dietary lutein intake lowers the risk of breast and stomach cancers. Lutein has toxic and suppressive effects on cancer cell lines, including those from the prostate, breast, hepatic, and cervical regions (Kavalappa, Y.P., 2020).

A carotenoid that is abundant in fruits and vegetables, lutein mostly builds up in the macular area of the human retina (Lei Fang, 2020). Because of its physiological benefits, including anti-inflammatory, antioxidant, antidepressant, and anti-angiogenic properties, lutein is useful in treating visual conditions such as cataracts, age-related macular degeneration, and DED. Lutein has a low bioavailability in humans because it is hydrophobic and sensitive to heat and light. Furthermore, lutein is easily oxidized and broken down, making storage and shipping more challenging (Jiang Yi, 2016). The breakdown of lutein in the stomach must be prevented, and the efficiency of lutein absorption at small intestinal sites must be increased, to increase the effectiveness of lutein in human consumption. Therefore, for the oral route of such lutein intervention, it is extremely desirable to design and prepare a delivery carrier to enhance the intestinal transport efficiency of lutein.

With benefits like enhanced stability, controlled release, and higher bioavailability, nanocarriers are being employed to improve the transport and efficacy of antioxidants. Antioxidants are encapsulated in spherical vesicles called liposomes, which are composed of lipid bilayers. Solid Lipid Nanoparticles (SLNs) are tiny particles with a solid lipid core that are utilized to release antioxidants under regulated conditions. Because of their more porous shape, nanostructured lipid carriers (NLCs) may improve the release of antioxidants. These types of conjugated nanoparticles are used in the medicine field for their long shelf life, stability, and targeted drug delivery. Lutein is most used in Ophthalmology, and this type of lutein-based conjugated NPs will surely aid in targeted drug delivery and stability of the medications. Because lipid-based nanoparticles can improve the stability, bioavailability, and targeted delivery of antioxidants, they are employed as carriers for their administration. Solid lipid nanoparticles (SLNs) and nanostructured lipid carriers (NLCs) are two examples of nanoparticles that encapsulate antioxidants, preventing their breakdown and enabling their passage through biological barriers. This method works especially well for nutraceuticals that are taken orally (Gonçalves C, 2021). Particularly in the retina, polymeric nanoparticles can enhance the absorption and distribution of lutein, an antioxidant carotenoid. Researchers have improved lutein's water affinity, stability, and bioavailability by encasing it in a polymeric matrix. To make lutein-loaded nanoparticles, some polymers such as PLGA, PEG, and chitosan have been utilized. Because they can encapsulate and protect the carotenoid, enhancing its bioavailability, lipid-based nanoparticles—in particular, Solid Lipid Nanoparticles (SLNs) and Nanostructured Lipid Carriers (NLCs)—are attractive lutein delivery vehicles. These methods improve the solubility and stability of lutein by forming a nanoscale matrix for it using lipids such as cocoa butter, palm oil, and other triglycerides (Algan, A. H., 2022). Due to its limited water solubility and fat solubility, lutein may be more difficult for the body to absorb and distribute. When lutein is encapsulated in polymeric nanoparticles, it becomes more soluble in water and may be delivered more effectively to concentrated tissues like the retina. Further increasing lutein's bioavailability, polymeric nanoparticles can shield it from enzymatic and other physiological degradation (Bolla PK, 2020).

Brassica oleracea (broccoli) is a vegetable that is commonly eaten around the globe. Broccoli contains a wide range of nutrients, vitamins (A and C), fibers, and isothiocyanates. Isothiocyanates are mainly generated by the hydrolysis of glucosinolates via myrosinase (Lafarga, T, 2018). Broccoli (Brassica oleracea L.) sprout, a cruciferous vegetable, is abundant in antioxidant vitamins and phenolic compounds, giving it strong antioxidant and anti-inflammatory properties. It contains significantly higher levels of glucoraphanin and indolic glucosinolates compared to broccoli florets [Westphal, A., 2017]. It has been reported that broccoli contains flavonols and hydroxycinnamoyl derivatives. Only a limited number of studies have been done on anthocyanins in broccoli, which represent the most significant category of plant pigments among the coloured flavonoids and exhibit strong antioxidant activity (AA) (Monero et al., 2010). According to Monero et al. (2010), who examined the characteristics of acylated anthocyanins in broccoli, purple-sprouting broccoli owes its color to anthocyanins. Hence, in our study, we aimed to conjugate lutein to the green synthesized copper nanoparticles and study their antioxidant potential.

2. Materials and methods

Study Material: Copper sulphate pentahydrate, DPPH, Ferrozine, and all the reagents used for the study are procured from Qualigens.

Preparation of extracts: We bought Brassica oleracea var. italic from a nearby vendor in Bangalore. Dust and other undesired dirt particles were removed by washing with distilled water. The flowers were separated from the main stem and sliced into little fragments. After being cut off from the main peduncle, the stalks were finely minced. The two pieces were exposed to the sun for two to three days. After the components were ground into a fine powder, filter sheets were used to filter them. Up until a fine, amorphous powder was achieved, filtering was continued. The powders were utilized in the following section for the green synthesis. After 50g of stem powder and 50g of florets are weighed separately, they are combined with 100 mL of deionized water and cooked for 20 to 30 minutes. To eliminate particle debris, the extracted material was first filtered using filter paper and then again using Whatman No. 1 filter paper. Until a clear solution was achieved, filtration was continued.

Green synthesis of Copper Nanoparticles: A 20 mM Copper (II) sulfate solution was added to an equal volume of extract (Florets and stalks). After stirring this combination for 24-48 hours, a colour shift was noticed. The solution was then centrifuged at 10,000rpm for 48hr, and the pellet obtained was dried at 80°C in a hot air oven (Bahareh Bakhshi, 2022). Following a thorough characterization with FTIR, the produced particles were then used for composite nanoparticle synthesis.

Lutein extraction: With a few minor adjustments, lutein extraction was carried out by Sachindra & Mahendrekar's (2005) description. To summarize, the extraction process involved mixing of 5gm of powdered florets with 200 mL of acetone and petroleum ether (50% v/v) for 24 hours at 40°C in a shaking water bath. The mixture was then back-washed with a 0.1% NaCl solution to separate the phases. After that, the mixture was centrifuged for 15 min at 8000 rpm (25°C). In a lyophilizer, the resulting supernatant was freeze-dried and stored at -20°C befoe being analysed.

Composite nanoparticle synthesis: The floret NPs (FNP) and stalk NPs (SNP) were used along with the lutein extracted in the previous step. The respective NPs were dissolved in deionized water and combined with an equal volume of lutein extract (5 mM). The solutions were placed magnetic stirrer at continuous shaking (40^0c rpm). Colour change was assumed during the NPs (FLNP and SLNP) synthesis. The particles were dried as described in the previous section.

Fourier transform infrared (FTIR) characterization: Fourier transform infrared (FTIR) spectra were collected using the KBr pellet method utilizing a Perkin Elmer Spectrum One FTIR spectrophotometer (Bomem MB100) with a 3600-400cm^{-1} range. All of the NPs synthesized (FNP, SNP, FLNP, SLNP) were characterized by FTIR. The pure lutein extract obtained was also characterized.

Antioxidant potential of the green synthesized NPs: The green synthesized NPs (FNP, SNP, L, FLNP, SLNP) were all evaluated for their potential antioxidant activity. Antioxidant ability was evaluated by DPPH free radical scavenging assay, hydrogen peroxide scavenging assay, reducing power (RP) method, and Ferrozine assay.

DPPH radical scavenging activity: The free radical scavenging ability of the NPs synthesized was estimated (Sreelekha et al., 2021) but with some modifications. The green synthesized NPs (All of the 5 test samples were used (FNP, SNP, L, FLNP, SLNP) were added to a solution of 1mM DPPH in ethanol at different concentrations (0, 25, 50, 100, 200, and 400µg/ml). To allow the NPs to interact with and scavenge DPPH radicals, the contents were vortexed and then incubated for 30 minutes at room temperature without light. A microplate reader (Genetix) was used to measure each solution's absorbance at 517nm, and the following formula was used to calculate the percentage of radical scavenging at each concentration. Higher levels of free radical activity in the reaction mixture are indicated by a lower absorbance value. Equation was used to determine the radical scavenging activity (%). Ascorbic acid (0.2mg/ml) was used as the positive control. Scavenging activity = (Absorbance of control – Absorbance of sample)/ Absorbance of control x 100.

Hydrogen peroxide scavenging assay: With certain changes, the extract's capacity to scavenge hydrogen peroxide (H_2O_2) was assessed using Bhatti, M.Z. et al (2015). The eppendorf tubes were filled with 0.1 mL of aliquots of green synthesized NPs (FNP, SNP, L, FLNP, and SLNP) at different concentrations (25–400µg/ml). The volume of the tubes was then increased to 0.4 mL using 50mM phosphate buffer (pH 7.4), and 0.6 mL of H_2O_2 solution (2 mM) was added. After vortexing the reaction mixture for 10 min, the absorbance at 230nm was measured using UV Spectroscopy (Shimadzu, 1800). As the positive control, ascorbic acid (0.2mg/ml) was employed. The following formula was used to determine the extracts' capacity to scavenge H_2O_2. H_2O_2 scavenging activity percentage = $[(A0-A1)/A0]\times100$; where: A_0 = Absorbance of control, A_1 = Absorbance of sample.

Reducing power method: With a few adjustments, the reducing power was calculated using the Kubavat, K., et al. (2022) approach. About 0.5 mL of phosphate buffer (0.2M, pH 6.6) and 0.5 mL of 1% potassium ferricyanide were combined individually with 0.2 mL aliquots of NPS (FNP, SNP, L, FLNP, and SLNP) at different concentrations (25–400µg/mL). For 20 min, the mixture was incubated at 50°C in a water bath and was allowed to cool to ambient temperature before being centrifuged for 10 min at 3,000 rpm with 0.5 mL of 10% trichloroacetic acid added. After collecting 0.5 mL of the supernatant, it was combined with 0.5 mL of distilled water. This was followed by the addition of 0.1 mL of 0.1% ferric chloride, the mixture was allowed to sit at room temperature for ten minutes. At 700nm, the absorbance was measured in a UV spectrophotometer (Shimadzu, 1800). Ascorbic acid was used as a positive control (0.2mg/ml).

Ferrozine assay: According to this technique, chelating compounds stabilize the oxidized state of the metal ion by lowering the redox potential, which makes them useful as secondary antioxidants. The synthesized nanoparticles (FNP, L, and FLNP) at varying concentrations (25 to 400µg/ml) were used to assess the iron-chelating activity of the particles. About 50µL of $FeCl_2$ (2 mM) and 100µL of ferrozine (FZ, 5 mM) were combined with 1 mL of the NPs and 3 mL of distilled water. The contents were mixed thoroughly and allowed to stand for 10 minutes. A UV-Vis spectrophotometer was then used to test the solution's OD at 562nm. The percentage inhibition of ferrozine Fe^{2+} complex was calculated by the following equation. FZ Fe^{2+} complex % = [(Acontrol - Asample)/Asample] × 100. Citric acid was used as a positive control.

Statistics Analysis: SPSS (faculty version) was used for the data analysis. Standard metrics like mean and standard deviation (SD) values were used. To determine the correlation between two quantitative variables, the Pearson correlation was calculated. To determine any potential relationships between the evaluation techniques, correlation analysis was performed.

3. Results

FTIR characterization: The FTIR measurements for the green synthesized copper NPs are shown in the figures below. This could aid in identifying the possible bio molecules that could act as reducing and capping agents. The strong peaks in FE spectra observed at 3450.56, 3250.81, 1686.54, 1580.23, 1424.56, 1056.43, 600.14 and 521.34cm^{-1}, which represent O–H, C–H, C=C, C=C, C=C, C–OH stretching's and C–OH bending and C–OH bending respectively (Sahu, N, 2013). The strong peaks in SE spectra observed at 3450.56, 1686.54, 1580.23, 1424.56, 1056.43, 600.14 and 521.34 cm-1, which represent alcoholic, C=C, C=C, C=C, C–OH stretchings and C–OH bending and C–OH bending respectively (Sahu, N, 2013). The bands at 521.34 cm-1 and 600.14 cm^{-1} might indicate the formation of Cu nanostructure and Cu–O stretching. The peak at 3450.56 might be due to an amino acid which acts as capping agent [Anand, T, 2012].

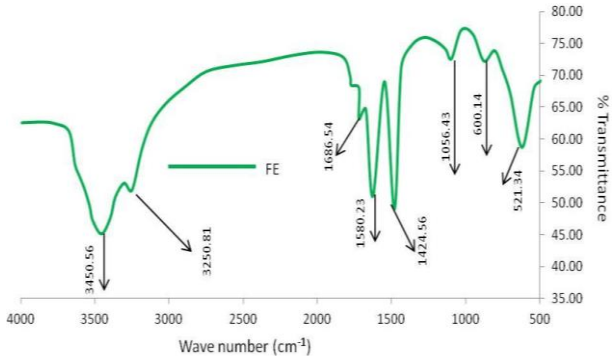

Fig. 1: Image Showing the FTIR Spectrum of the Green Synthesized CuNPs with Floret Extract (FE) Showing the Bands of the Groups.

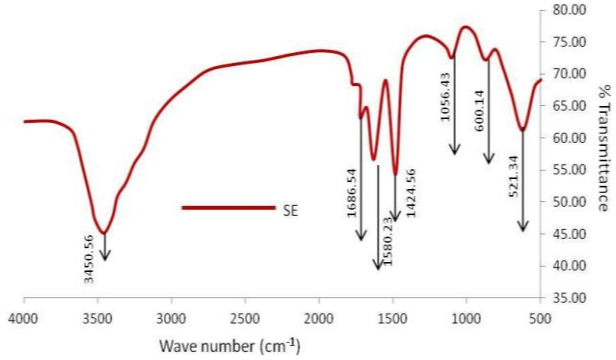

Fig. 2: Image Showing the FTIR Spectrum of the Green Synthesized CuNPs with Stalk Extract (SE).

Structural Characterization of Lutein in the Nanoparticles by FTIR: FTIR verified that the lutein extract was stable in the NPs. Figure displays the FTIR spectra of the lutein NPs from the stalk and florets, as well as the lutein removed from the florets in the preceding stage. They provide details on the lutein extract's molecular structures in the lutein nanoparticles. At 2921cm^{-1} and 2856cm^{-1}, the distinctive bands of the lutein reference emerged, signifying the symmetric and asymmetric vibrations of CH_2 and CH_3. The adsorption band located at 3432 cm-1 is attributed to hydrogen bonding between molecules. Similarities in the functional group environment are suggested by the frequencies, which are close to those obtained with the lutein. Thus, at 0 weeks of storage, the FTIR measurements confirm the molecular structure of the lutein in the lutein NPs.

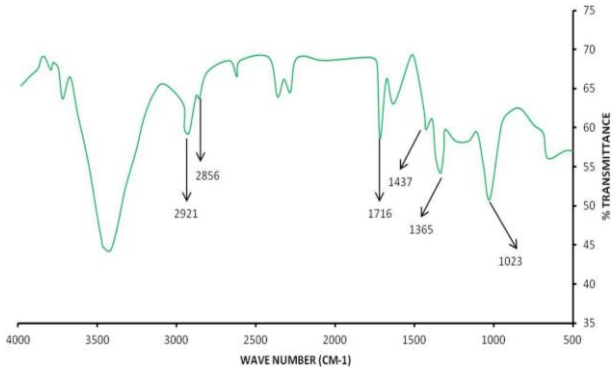

Fig. 3: Image Showing the FTIR Spectrum of the Lutein Extract Extracted. Lutein Showing the Absorption Peaks of the Functional Groups at 2921, 2856, 1716, 1437, 1365 and 1023.

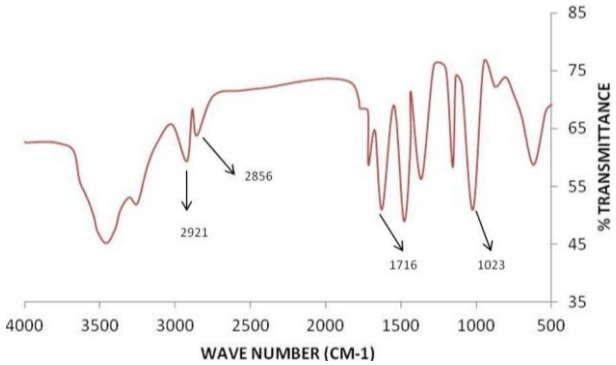

Fig. 4: FLNP: Image Showing the FTIR Spectrum of the Green Synthesized CuNPs with Florets Extract (FE) and Lutein. The characteristic Peaks of 2921, 2856, 1716, and 1023 Can Be Seen in the Spectra.

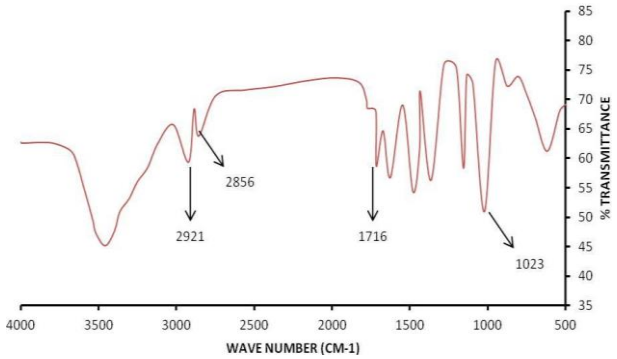

Fig. 5: SLNP: Image Showing the FTIR Spectrum of the Green Synthesized CuNPs with Stalk Extract (SE) and Lutein. The characteristic Peaks of 2921, 2856, 1716, and 1023 Can Be Seen in the Spectra.

4. Antioxidant potential assay

DPPH scavenging assay: The antioxidant potential of CuNPs was evaluated by the DPPH method using NPs having IC_{50} of 30.04µg/ml. From our data, we found FLNP to be highly antioxidant, followed by FNP, when compared to the positive control. FLNP and FNP showed 92 and 88% scavenging of DPPH free radicals, respectively, at 400µg/ml concentrations. On the other hand positive control showed 95% scavenging, while only lutein extract showed 67% scavenging. The IC50 of the FNP, SNP, L, FLNP, and SLNP were found to be 94.33, 142.85, 113.63, 68.4, and 128.2µg/ml, respectively. FLNP showed the lowest IC50 when compared to the positive control (58.65µg/ml).

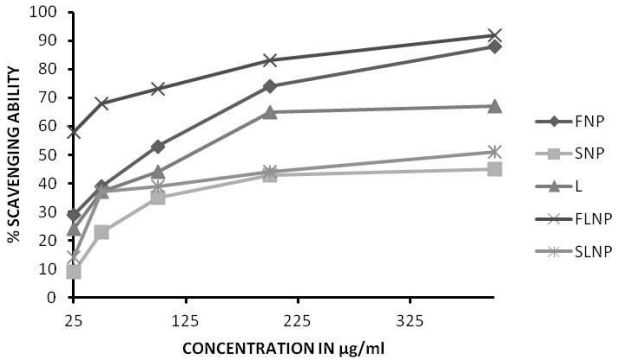

Fig. 6: DPPH Scavenging Assay: Graph Showing the % Scavenging Ability of the Extracts on DPPH. Positive Control Was Found to Be 95%. Not Shown in the Graph.

Hydrogen peroxide scavenging assay: The scavenging effect on hydrogen peroxide was found to be concentration-dependent (25–400µg/ml) ($P < 0.05$). The methanol:water extract is said to exhibit a good H_2O_2 scavenging activity (IC_{50} 43.53µg/ml). [Water extract exhibited IC_{50} 51.27µg/ml). The significant difference in percentage inhibition of H_2O_2 of all the NPs was compromising in Figure 1 $P < 0.05$. Among various NPs, FLNP showed good H_2O_2 scavenging activity (IC_{50} 72.55µg/ml), followed by FNP when compared to the positive control. FLNP and FNP showed 78 and 69%, respectively, at 400µg/ml. On the other hand, positive control showed 78% scavenging at 200µg/ml. Lutein showed scavenging of 62% ($p<0.05$). The IC50 of the FNP, SNP, L, FLNP, and SLNP were found to be 147.05, 156.25, 119.04, 96.15,and 208.33µg/ml, respectively. FLNP showed the lowest IC50 when compared to the positive control (76.92µg/ml).

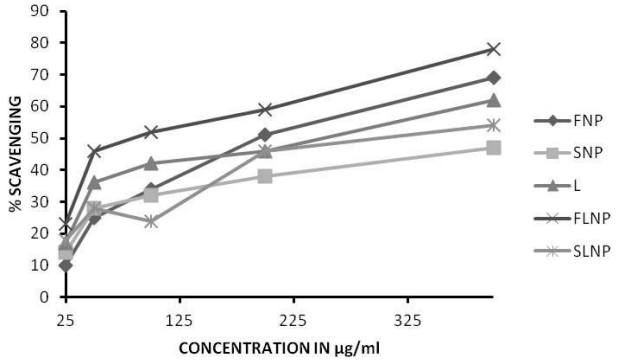

Fig. 7: H_2O_2 Scavenging Assay: Graph Showing the % Scavenging Ability of the Extracts on Hydrogen Peroxide. Positive Control Was Found to Be 78%.

Reducing power method: A rise in OD value represents the strength of antioxidant activity. The FLNP showed dose-dependent absorbance. At 400µg/ml, FLNP, FNP, and Lutein showed 94, 91 and 87% antioxidant capacity when compared to the positive control. On the other hand, positive control showed 93% antioxidant ability at 200µg/ml ($P<0.05$). The IC50 of the FNP, L, and FLNP were found to be 102.3, 145.36, and 87.5µg/ml, respectively. FLNP showed the lowest IC50 when compared to the positive control (63.45µg/ml).

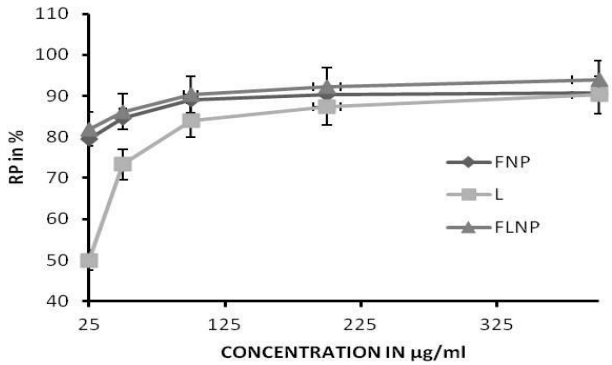

Fig. 8: Reducing Power Assay: Graph Showing the Reducing Power at 700nm of the Green Synthesized NPs. Positive Control Was 93% at 200µg/mL.

Ferrozine assay: Our results reveal that FLNP showed good iron binding, confirming its role as an antioxidant. FLNP and FNP exhibited 92% and 88% FZ reduction ability, respectively, which is proportional to the antioxidant ability. Citric acid displayed very strong activity of 89% at 200µg/ml ($P<0.05$). On the other hand, lutein exhibited 67% at 200µg/ml ($P<0.05$). The iron chelating activity of FLNP has been reported to be very high when compared to other samples and the positive control. The IC50 of the FNP, L, and FLNP were found to be 134, 231, and 99µg/ml, respectively. FLNP showed the lowest IC50 when compared to the positive control (82.34µg/ml). By building chelates with Fe2+, ferrozine can generate a red complex. The red coloured complexes formed are reduced because of this reaction, which is limited when other chelating agents are present. The metal chelating activity is measured by the colour decrease.

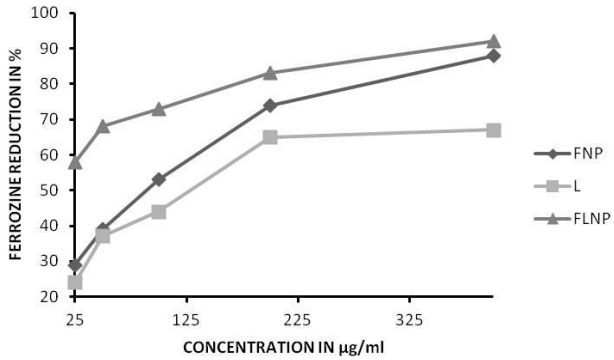

Fig. 9: Ferrozine Reduction Assay: Graph Showing the Ferrozine Reduction in % at 562nm of the Green Synthesized CuNPs. Positive Control Showed 89% Inhibition.

Correlation between the methods of antioxidant evaluation: The link between different methods of antioxidant evaluation was investigated using correlation analysis. Highly positive associations were found between FZ and RP method (r=0.99995), FZ and DPPH method (r=0.93963), and DPPH and RP method (r=0.93615). A weak correlation was seen between hydrogen peroxide and the DPPH method (r=0.522702).

5. Discussion

The characteristic lutein absorption bands appeared at 2921cm^{-1} and 2856cm^{-1}, indicating the symmetric and asymmetric stretches of CH_2 and CH_3. Molecular structure of the lutein component in the synthesized NPs is thus confirmed by the FTIR tests at 0 weeks of storage. Similar types of peaks were reported by Adela, Mora-Gutierrez (2022) at 2924 and 2852cm^{-1}. At 1718, the distinctive band representing the C=O stretching vibrations is located. Our findings at FTIR are in line with these reference findings. We found lutein peaks of the groups at 2921, 2856, 1716, 1437, 1365, and 1023cm^{-1}. Similar banding patterns were also discovered by Manzoor, Shaziya, et al. (2022) when they used ultrasound-assisted extraction (UAE) to remove the petals of marigold flowers. They noted notable lutein peaks at 3253, 2928, 1588, 1269, and 1018 cm^{-1}. The C–H vibrations are represented by the peaks at 2928 and 3253cm^{-1}. The C = O vibrations are indicated by bands at 1588 cm^{-1} (J. Huang, 2019).

Egg yolks and dark green leafy vegetables are two examples of foods that contain lutein, a xanthophyll pigment. Due to its antioxidant properties, lutein scavenges reactive oxygen species, including lipid peroxy radicals and singlet oxygen. Inflammatory mediators are triggered by oxidative stress, which results in the emergence of inflammatory and metabolic disorders (Ahn YJ, 2021).

From our evaluation assays, we found FLNP to be highly antioxidant. CuNPs' strong antioxidant capacity was assessed using the DPPH radical scavenging assay, which had an IC50 of 30.04µg/mL. When compared to the positive control, our data showed that FLNP was the most antioxidant, followed by FNP. At 400µg/ml concentrations, FLNP and FNP demonstrated 92 and 88% DPPH free radical scavenging, respectively. However, only lutein extract demonstrated 67% scavenging, whereas the positive control demonstrated 95% scavenging. Similar reports were seen from Bhattacharyya S, (2010) in a linoleic acid emulsion system, measurements were made of the total antioxidant capacity, reducing power, hydroxyl, DPPH, and ABTS (*+) radical scavenging activities, iron chelation capacity, and prevention of lipid peroxidation. Lutein was found to be an antioxidant in nature as extracted from several vegetables and fruits. According to studies by Ingkasupart et al. (2015) and Bhattacharyya et al. (2010), which analyzed the antioxidant activities and lutein content of marigold cultivars, some of them had both high antioxidant activities and high lutein content. On the other hand, some of the cultivars showed high antioxidant activities but not high lutein content, and vice versa. These findings suggest that a plant's high lutein concentration does not necessarily translate into significant antioxidant activity. Furthermore, according to Burgos et al. (2013), spinach is a rich source of lutein. It did, however, demonstrate lutein's poor rate of bioaccessibility. The bioavailability of lutein was lowest in green foods (broccoli and spinach) and highest in non-green vegetables (carrot, tomato paste, and red pepper). However, no reports were found where copper nanoparticles conjugated with lutein exhibited antioxidant potential. To our knowledge, we claim the first manuscript to report the previously mentioned

statement. Due to its therapeutic effectiveness in preventing disease, lutein has been reviewed and addressed in the literature regularly (Arunkumar R., 2020). However, there has been little focus on lutein distribution through innovative drug delivery systems, particularly inside nanocarriers (Wong K.-H., 2022).

Conclusion: Broccoli florets and stalk extracts contained some amount of lutein, yet each part has a unique antioxidant activity. The antioxidant activity of CuNPs synthesized from florets and conjugated with lutein extract exhibited high antioxidant activity when compared to stalks and their associated NPs. Lutein's exceptional light-absorbing capabilities are caused by its long double-bond system and the OH groups attached to the chromophore. Its distinct structure is thought to be the cause of anti-oxidant properties, as well as its capacity to prevent the onset of degenerative diseases like cancer, atherosclerosis, and neurodegenerative diseases, in addition to ocular conditions like AMD and cataracts. Furthermore, the development and manufacturing of nanoparticles for encapsulating naturally occurring bioactive chemicals to improve their stability. Comprehensive clinical studies should be conducted to assess the potential of nanotechnology-based techniques for lutein administration. The hopeful results of recent advancements in the field of nanotechnology have been made public. The economic nature of technologies continues to be a critical factors in their success. Enhancing lutein's therapeutic efficacy and clinical translation will be made possible by the growing success of nanoscale delivery technologies.

References

[1] Adela, Mora-Gutierrez & Marquez, Sixto & Attaie, Rahmat & Nunez de Gonzalez, Maryuri & Jung, Yoonsung & Woldesenbet, Selamawit & Moussavi, Mahta. (2022). Mixed Biopolymer Systems Based on Bovine and Caprine Caseins, Yeast β-Glucan, and Maltodextrin for Microencapsulating Lutein Dispersed in Emulsified Lipid Carriers. Polymers. 14. 2600. https://doi.org/10.3390/polym14132600.

[2] Ahn YJ, Kim H. Lutein as a Modulator of Oxidative Stress-Mediated Inflammatory Diseases. Antioxidants (Basel). 2021 Sep 13;10(9):1448. doi: 10.3390/antiox10091448. PMID: 34573081; PMCID: PMC8470349. https://doi.org/10.3390/antiox10091448.

[3] Algan, A. H., Gungor-Ak, A., & Karatas, A. (2022). Nanoscale Delivery Systems of Lutein: An Updated Review from a Pharmaceutical Perspective. *Pharmaceutics*, *14*(9), 1852. https://doi.org/10.3390/pharmaceutics14091852.

[4] Arunkumar R., Gorusupudi A., Bernstein P.S. The macular carotenoids: A biochemical overview. Biochim. Biophys. Acta Mol. Cell Biol. Lipids. 2020; 1865:158617. https://doi.org/10.1016/j.bbalip.2020.158617.

[5] Bhattacharyya S, Datta S, Mallick B, Dhar P and Ghosh S 2010 J. Agric. Food Chem. 58, 8259- 64. https://doi.org/10.1021/jf101262e.

[6] Bhattacharyya S, Datta S, Mallick B, Dhar P, Ghosh S. Lutein content and in vitro antioxidant activity of different cultivars of Indian marigold flower (Tagetes patula L.) extracts. J Agric Food Chem. 2010 Jul 28;58(14):8259-64. https://doi.org/10.1021/jf101262e.

[7] Bhatti, M.Z., Ali, A., Ahmad, A. *et al.* Antioxidant and phytochemical analysis of *Ranunculus arvensis* L. extracts. *BMC Res Notes* 8, 279 (2015). https://doi.org/10.1186/s13104-015-1228-3.

[8] Blazquez S, Olmos E, Hernandez JA, Fernandez-Garcıa N, Fernandez JA, Piqueras A (2009) Somatic embryogenesis in saffron (Crocus sativus L.) Histological differentiation and implication of some components of the antioxidant enzymatic system. Plant Cell Tiss Organ Cult 97:49–57 https://doi.org/10.1007/s11240-009-9497-y.

[9] Boligon AA, Pereira RP, Feltrin AC, Machado MM, Janovik V, Rocha JBT et al (2009) Antioxidant activities of flavonol derivatives from the leaves and stem bark of Scutia buxifolia Reiss. Bioresour Technol 100:6592–6598 https://doi.org/10.1016/j.biortech.2009.03.091.

[10] Bolla PK, Gote V, Singh M, Patel M, Clark BA, Renukuntla J. Lutein-Loaded, Biotin-Decorated Polymeric Nanoparticles Enhance Lutein Uptake in Retinal Cells. Pharmaceutics. 2020 Aug 24;12(9):798. https://doi.org/10.3390/pharmaceutics12090798.

[11] Brownie S. (2006). Why are elderly individuals at risk of nutritional deficiency? 12 110–118. https://doi.org/10.1111/j.1440-172X.2006.00557.x.

[12] Burgos G, Muñoa L, Sosa P, Bonierbale M, zum Felde T and Díaz C 2013 In vitro bioaccessibility of lutein and zeaxanthin of yellow fleshed boiled potatoes Plant Foods for Human Nutrition 68 385–390. https://doi.org/10.1007/s11130-013-0381-x.

[13] Chung H. Y., Cesari M., Anton S., Marzetti E., Giovannini S., Seo A. Y., et al. (2009). Molecular inflammation: underpinnings of aging and age-related diseases. 8 18–30. https://doi.org/10.1016/j.arr.2008.07.002.

[14] Eliassen, A.H.; Hendrickson, S.J.; Brinton, L.A.; Buring, J.E.; Campos, H.; Dai, Q.; Dorgan, J.F.; Franke, A.A.; Gao, Y.T.; Goodman, M.T.; et al. Circulating carotenoids and risk of breast cancer: Pooled analysis of eight prospective studies. *J. Natl. Cancer Inst.* 2012, *104*, 1905–1916. https://doi.org/10.1093/jnci/djs461.

[15] Eliassen, A.H.; Liao, X.; Rosner, B.; Tamimi, R.M.; Tworoger, S.S.; Hankinson, S.E. Plasma carotenoids and risk of breast cancer over 20 y of follow-up. *Am. J. Clin. Nutr.* 2015, *101*, 1197–1205. https://doi.org/10.3945/ajcn.114.105080.

[16] Gonçalves C, Ramalho MJ, Silva R, Silva V, Marques-Oliveira R, Silva AC, Pereira MC, Loureiro JA. Lipid Nanoparticles Containing Mixtures of Antioxidants to Improve Skin Care and Cancer Prevention. Pharmaceutics. 2021 Nov 30;13(12):2042. https://doi.org/10.3390/pharmaceutics13122042.

[17] Ingkasupart P, Manochai B, Song W T and Hong J H 2015 Food Sci. Technol. 35 380-5. https://doi.org/10.1590/1678-457X.6663.

[18] J. Huang, F. Bai, Y. Wu, Q. Ye, D. Liang, C. Shi, X. Zhang, Development and evaluation of lutein-loaded alginate microspheres with improved stability and antioxidant, Journal of the Science of Food and Agriculture. 99 (2019) 5195–5201, https://doi.org/10.1002/jsfa.9766.

[19] Jiang Yi, Yuting Fan, Wallace Yokoyama, Yuzhu Zhang, Liqing Zhao, Characterization of milk proteins–lutein complexes and the impact on lutein chemical stability, Food Chemistry, Volume 200, 2016, Pages 91-97. https://doi.org/10.1016/j.foodchem.2016.01.035.

[20] Kandola K., Bowman A., Birch-Machin M. A. (2015). Oxidative stress–a key emerging impact factor in health, ageing, lifestyle and aesthetics. 37(Suppl. 2) 1–8. https://doi.org/10.1111/ics.12287.

[21] Kang J. H., Ascherio A., Grodstein F. (2005). Fruit and vegetable consumption and cognitive decline in aging women. 57 713–720. https://doi.org/10.1002/ana.20476.

[22] Kavalappa, Y.P.; Gopal, S.S.; Ponesakki, G. Lutein inhibits breast cancer cell growth by suppressing antioxidant and cell survival signals and induces apoptosis. *J. Cell Physiol.* 2020, *236*, 1798–1809. https://doi.org/10.1002/jcp.29961.

[23] Kim, J.H.; Lee, J.; Choi, I.J.; Kim, Y.I.; Kwon, O.; Kim, H.; Kim, J. Dietary carotenoids intake and the risk of gastric cancer: A Case Control study in Korea. *Nutrients* 2018, *10*, 1031. https://doi.org/10.3390/nu10081031.

[24] Kregel K. C., Zhang H. J. (2007). An integrated view of oxidative stress in aging: basic mechanisms, functional effects, and pathological considerations. 292 R18–R36. https://doi.org/10.1152/ajpregu.00327.2006.

[25] Kubavat, K., Trivedi, P., Ansari, H. *et al.* green synthesis of silver nanoparticles using dietary antioxidant rutin and its biological contour. *Beni-Suef Univ J Basic Appl Sci* 11, 115 (2022). https://doi.org/10.1186/s43088-022-00297-x.

[26] Kulisic T, Radonic A, Katalinic V, Milos M (2004) Use of different methods for testing antioxidative activity of oregano essential oil. Food Chem 85:633–640 https://doi.org/10.1016/j.foodchem.2003.07.024.

[27] Lafarga, T.; Bobo, G.; Viñas, I.; Collazo, C.; Aguiló-Aguayo, I. Effects of thermal and non-thermal processing of cruciferous vegetables on glucosinolates and its derived forms. *J. Food Sci. Technol.* 2018, *5*, 1973–1981. https://doi.org/10.1007/s13197-018-3153-7.

[28] Lei Fang, Hua Lin, Zhenfeng Wu, Zhen Wang, Xinxin Fan, Ziting Cheng, Xiaoya Hou, Daquan Chen, In vitro/vivo evaluation of novel mitochondrial targeting charge-reversal polysaccharide-based antitumor nanoparticle, Carbohydrate Polymers, Volume 234, 2020, 115930 https://doi.org/10.1016/j.carbpol.2020.115930.

[29] Manzoor, Shaziya & Rashid, Rubiya & Panda, Bibhu & Sharma, Vasudha & Azhar, Mohd. (2022). Green extraction of Lutein from Marigold flower petals, process optimization and its potential to improve the oxidative stability of sunflower oil. Ultrasonics Sonochemistry. 85. https://doi.org/10.1016/j.ultsonch.2022.105994.

[30] Monero, D. A., Perez-Balibrea, S., Ferreres, F. et al. (2010) Acylated anthocyanins in broccoli sprouts, Food Chemistry, 123 (2), 358–363. https://doi.org/10.1016/j.foodchem.2010.04.044.
[31] Muller O., Krawinkel M. (2005). Malnutrition and health in developing countries. 173 279–286. https://doi.org/10.1503/cmaj.050342.
[32] N.M. Sachindra, N.S. Mahendrakar, Process optimization for extraction of carotenoids from shrimp waste with vegetable oils, Bioresource Technology. 96 (2005) 1195–1200, https://doi.org/10.1016/j.biortech.2004.09.018.
[33] Nagata C., Nakamura K., Wada K., Oba S., Hayashi M., Takeda N., et al. (2010). Association of dietary fat, vegetables and antioxidant micronutrients with skin ageing in Japanese women. 103 1493–1498. https://doi.org/10.1017/S0007114509993461.
[34] Prieto P, Pineda M, Aguliar M (1999) Spectrophotometric quantitation of antioxidant capacity through the formation of phosphomolybdenum complex: specific application to the determination of vitamin E. Anal Biochem 269:337–34 https://doi.org/10.1006/abio.1999.4019.
[35] Rogers N. M., Seeger F., Garcin E. D., Roberts D. D., Isenberg J. S. (2014). Regulation of soluble guanylate cyclase by matricellular thrombospondins: implications for blood flow. 5:134. https://doi.org/10.3389/fphys.2014.00134.
[36] Ruch RJ, Cheng SJ, Klaunig JE (1989) Prevention of cytotoxicity and inhibition of intercellular communication by antioxidant catechins isolated from Chinese green tea. Carcinogenesis 10:1003–1008 https://doi.org/10.1093/carcin/10.6.1003.
[37] Shah SMM, Sadiq A, Shah SMH, Ullah F (2014) Antioxidant, total phenolic contents and antinociceptive potential of Teucrium stocksianum methanolic extract in different animal models. BMC Complement Altern Med. 14:181 https://doi.org/10.1186/1472-6882-14-181.
[38] Sikder MAA, Rahman MA, Islam MR, Abul KM, Kiasar MA, Rahman MS et al (2010) In-vitro antioxidant, reducing power, free radical scavenging and membrane stabilizing activities of Spilanthes calva. Bangladesh Pharmaceut J. 13:63–67
[39] Sreelekha, E., George, B., Shyam, A., Sajina, N., and Mathew, B. (2021). A comparative study on the synthesis, characterization, and antioxidant activity of green and chemically synthesized silver nanoparticles. *Bionanoscience* 11, 489–496. https://doi.org/10.1007/s12668-021-00824-7.
[40] Trachootham D, Lu W, Ogasawara MA, Nilsa RD, Huang P. Redox regulation of cell survival Antioxid Redox Signal. 2008; 10:1343–74 https://doi.org/10.1089/ars.2007.1957.
[41] Trifunovic A., Wredenberg A., Falkenberg M., Spelbrink J. N., Rovio A. T., Bruder C. E., et al. (2004). Premature ageing in mice expressing defective mitochondrial DNA polymerase. 429 417–423. https://doi.org/10.1038/nature02517.
[42] Valko M, Rhodes CJ, Moncol J, Izakovik M, Mazure M. Free radicals, metals and antioxidants in oxidative stress-induced cancer Chem Biol Interact. 2006; 160:1–40 https://doi.org/10.1016/j.cbi.2005.12.009.
[43] Vinardell, M. P., & Mitjans, M. (2015). Nanocarriers for Delivery of Antioxidants on the Skin. *Cosmetics*, *2*(4), 342-354. https://doi.org/10.3390/cosmetics2040342 https://doi.org/10.3390/cosmetics2040342.
[44] Westphal, A.; Riedl, K.M.; Cooperstone, J.L.; Kamat, S.; Balasubramaniam, V.M.; Schwartz, S.J.; Böhm, V. High-pressure processing of broccoli sprouts: Influence on bioactivation of glucosinolates to isothiocyanates. *J. Agric. Food. Chem.* 2017, *65*, 8578–8585. https://doi.org/10.1021/acs.jafc.7b01380.
[45] Weydert C.J., Cullen J.J. Measurement of superoxide dismutase, catalase and glutathione peroxidase in cultured cells and tissue. *Nat. Protoc.* 2010; 5: 51–66. https://doi.org/10.1038/nprot.2009.197.
[46] Wong K.-H., Nam H.-Y., Lew S.-Y., Naidu M., David P., Kamalden T.A., Hadie S.N.H., Lim L.-W. Discovering the Potential of Natural Antioxidants in Age-Related Macular Degeneration: A Review. Pharmaceuticals. 2022; 15: 101. https://doi.org/10.3390/ph15010101.
[47] Zhang, D. and Hamauzu, Y. (2004) Phenolics, ascorbic acid, carotenoids and antioxidant activity of broccoli and their changes during conventional and microwave cooking, Food Chemistry, 88 (4), 503–509. https://doi.org/10.1016/j.foodchem.2004.01.065.
[48] Zhou T., Prather E. R., Garrison D. E., Zuo L. (2018). Interplay between ROS and antioxidants during ischemia-reperfusion injuries in cardiac and skeletal muscle. 19: E417. https://doi.org/10.3390/ijms19020417.
[49] Zur I, Dubas E, Krzewska M, Janowiak F, Hura K, Pociecha E et al (2014) Antioxidant activity and ROS tolerance in triticale (xTriticosecale Wittm.) anthers affect the efficiency of microspore embryogenesis. Plant Cell Tiss Organ Cult. https://doi.org/10.1007/s11240-014-0515-3.